

ON THE BLENDING OF REGULARIZATION AND LARGE-EDDY SIMULATION MODELS

David Folch¹, F.Xavier Trias¹, Andrey Gorobets^{1,2} and Assensi Oliva¹

¹Heat and Mass Transfer Technological Center, Technical University of Catalonia
ETSEIAT, C/Colom 11, 08222 Terrassa, Spain

²Keldysh Institute of Applied Mathematics, 4A, Miusskaya Sq., Moscow 125047, Russia

Key words: Regularization, Large-eddy simulation, Turbulence

Abstract. Direct simulations of the incompressible Navier-Stokes equations at high Reynolds numbers are not feasible because the convective term produces far too many relevant scales of motion. Therefore, in the foreseeable future, numerical simulations of turbulent flows will have to resort to models of the small scales. Large-eddy simulation (LES) and regularizations of the non-linear convective term are examples thereof. In the present work, we propose a natural blending between both approaches: restoring the Galilean invariance of the regularization method leads to an additional hyper-viscosity term that can be viewed as a LES model. Technical details such as the determination of the filter length and the balancing between regularization and LES are analyzed and discussed. Finally, the performance of the method is assessed through application to the Burgers' equation and a homogeneous isotropic turbulence.

1 INTRODUCTION

The incompressible Navier-Stokes (NS) equations form an excellent mathematical model for turbulent flows. In primitive variables they read

$$\partial_t \mathbf{u} + \mathcal{C}(\mathbf{u}, \mathbf{u}) = \mathcal{D}\mathbf{u} - \nabla p; \quad \nabla \cdot \mathbf{u} = 0, \quad (1)$$

where \mathbf{u} denotes the velocity field, p represents the pressure, the non-linear convective term is defined by $\mathcal{C}(\mathbf{u}, \mathbf{v}) = (\mathbf{u} \cdot \nabla) \mathbf{v}$ and the diffusive term reads $\mathcal{D}\mathbf{u} = \nu \Delta \mathbf{u}$, where ν is the kinematic viscosity. Since direct numerical simulations (DNS) of turbulent flows cannot be computed at high Reynolds numbers, a dynamically less complex mathematical formulation is needed. The most popular example thereof is the Large-Eddy Simulation (LES). Alternatively, regularizations of the non-linear convective term basically reduce the transport towards the small scales: the convective term in the NS equations, \mathcal{C} , is replaced by a smoother approximation [1, 2, 3]. In our previous works (see [4] and references therein), we restricted ourselves to the \mathcal{C}_4 approximation [3]: the convective term in the

NS equations (1) is replaced by the following $\mathcal{O}(\epsilon^4)$ -accurate smoother approximation

$$\mathcal{C}_4(\mathbf{u}, \mathbf{v}) = \mathcal{C}(\bar{\mathbf{u}}, \bar{\mathbf{v}}) + \overline{\mathcal{C}(\bar{\mathbf{u}}, \mathbf{v}')} + \overline{\mathcal{C}(\mathbf{u}', \bar{\mathbf{v}})}, \quad (2)$$

where the prime indicates the residual of the filter, *e.g.* $\mathbf{u}' = \mathbf{u} - \bar{\mathbf{u}}$, which can be explicitly evaluated, and $\overline{(\cdot)}$ represents a symmetric linear filter with filter length ϵ . However, two main drawbacks were observed: (i) due to the energy conservation, the model solution tends to display an additional hump in the tail of the spectrum (see Figures 2 and 3 in Section 4) and (ii) for very coarse meshes the damping factor can eventually take very small values.

In this context, we propose to combine regularization and LES modeling. The linkage follows from (approximately) restoring the Galilean invariance for the regularization by means of a modification of the diffusive term. For details the reader is referred to [5]. Shortly, by imposing all the symmetries and conservation properties of the original convective operator, $\mathcal{C}(\mathbf{u}, \mathbf{u})$, and canceling the second-order terms leads to the following one-parameter fourth-order regularization

$$\partial_t \mathbf{u}_\epsilon + \mathcal{C}_4^\gamma(\mathbf{u}_\epsilon, \mathbf{u}_\epsilon) = \mathcal{D}_4^\gamma \mathbf{u}_\epsilon - \nabla p_\epsilon; \quad \nabla \cdot \mathbf{u}_\epsilon = 0, \quad (3)$$

where the convective and the diffusive terms are modified in the same vein

$$\mathcal{C}_4^\gamma(\mathbf{u}, \mathbf{v}) = \frac{1}{2}((\mathcal{C}_4 + \mathcal{C}_6) + \gamma(\mathcal{C}_4 - \mathcal{C}_6))(\mathbf{u}, \mathbf{v}) \quad \text{and} \quad \mathcal{D}_4^\gamma \mathbf{u} = \mathcal{D} \mathbf{u} + \tilde{\gamma}(\mathcal{D} \mathbf{u})', \quad (4)$$

where $\tilde{\gamma} = 1/2(1 + \gamma)$ and $\mathcal{C}_6(\mathbf{u}, \mathbf{v}) = \mathcal{C}(\bar{\mathbf{u}}, \bar{\mathbf{v}}) + \mathcal{C}(\bar{\mathbf{u}}, \mathbf{v}') + \mathcal{C}(\mathbf{u}', \bar{\mathbf{v}}) + \overline{\mathcal{C}(\mathbf{u}', \mathbf{v}')}$. Notice that in this case the dissipation is reinforced by means of an hyper-viscosity term. As expected, this basically acts at the tail of the energy spectrum; therefore, it helps to mitigate the two above-mentioned drawbacks. From a LES point-of-view, we can relate the $\mathcal{C}\mathcal{D}_4^\gamma$ regularization to a closure models for any invertible filter. Then, to apply the method two parameters still need to be determined; namely, the local filter length, ϵ , and the constant $\tilde{\gamma}$. The former follows from the criterion that the vortex-stretching mechanism must stop at the smallest grid scale. The latter is approximately bounded by assuming that the smallest grid scale lies within the inertial range for a classical Kolmogorov energy spectrum. These issues are addressed in Sections 2 and 3, respectively. Then, the performance of the method is assessed through application to the Burgers' equation and a homogeneous isotropic turbulence in Section 4. Finally, relevant results are summarized and conclusions are given.

2 STOPPING THE VORTEX-STRETCHING MECHANISM

2.1 Interscale interactions

To study the interscale interactions in more detail, we continue in the spectral space. The spectral representation of the convective term in the NS equations is given by

$$\mathcal{C}(\mathbf{u}, \mathbf{u})_{\mathbf{k}} = i\Pi(\mathbf{k}) \sum_{\mathbf{p}+\mathbf{q}=\mathbf{k}} \hat{\mathbf{u}}_{\mathbf{p}} \mathbf{q} \hat{\mathbf{u}}_{\mathbf{q}}, \quad (5)$$

where $\Pi(\mathbf{k}) = I - \mathbf{k}\mathbf{k}^T/|\mathbf{k}|^2$ denotes the projector onto divergence-free velocity fields in the spectral space. Taking the Fourier transform of Eqs.(3), we obtain the evolution of each Fourier-mode $\hat{\mathbf{u}}_{\mathbf{k}}(t)$ of $\mathbf{u}_{\epsilon}(t)$ for the $\{\mathcal{CD}\}_4^\gamma$ approximation

$$\left(\frac{d}{dt} + h_4^\gamma(\widehat{G}_{\mathbf{k}})\nu|\mathbf{k}|^2\right)\hat{\mathbf{u}}_{\mathbf{k}} + i\Pi(\mathbf{k})\sum_{\mathbf{p}+\mathbf{q}=\mathbf{k}}f_4^\gamma(\widehat{G}_{\mathbf{k}},\widehat{G}_{\mathbf{p}},\widehat{G}_{\mathbf{q}})\hat{\mathbf{u}}_{\mathbf{p}}\mathbf{q}\hat{\mathbf{u}}_{\mathbf{q}} = \mathbf{F}_{\mathbf{k}}, \quad (6)$$

where $\widehat{G}_{\mathbf{k}}$ denotes the \mathbf{k} -th Fourier-mode of the kernel of the convolution filter, *i.e.*, $\widehat{\mathbf{u}}_{\mathbf{k}} = \widehat{G}_{\mathbf{k}}\hat{\mathbf{u}}_{\mathbf{k}}$. Notice that hereafter, for simplicity, the subindex ϵ is dropped. The mode $\hat{\mathbf{u}}_{\mathbf{k}}$ interacts only with those modes whose wavevectors \mathbf{p} and \mathbf{q} form a triangle with the vector \mathbf{k} . Thus, compared with Eq.(5), every triad interaction is multiplied by

$$f_4^\gamma(\widehat{G}_{\mathbf{k}},\widehat{G}_{\mathbf{p}},\widehat{G}_{\mathbf{q}}) = 1/2\{(1+\gamma)f_4 + (1-\gamma)f_6\}(\widehat{G}_{\mathbf{k}},\widehat{G}_{\mathbf{p}},\widehat{G}_{\mathbf{q}}), \quad (7)$$

where the f_4 and f_6 are given by

$$f_4(\widehat{G}_{\mathbf{k}},\widehat{G}_{\mathbf{p}},\widehat{G}_{\mathbf{q}}) = \widehat{G}_{\mathbf{k}}\widehat{G}_{\mathbf{p}} + \widehat{G}_{\mathbf{k}}\widehat{G}_{\mathbf{q}} + \widehat{G}_{\mathbf{p}}\widehat{G}_{\mathbf{q}} - 2\widehat{G}_{\mathbf{k}}\widehat{G}_{\mathbf{p}}\widehat{G}_{\mathbf{q}}, \quad (8)$$

$$f_6(\widehat{G}_{\mathbf{k}},\widehat{G}_{\mathbf{p}},\widehat{G}_{\mathbf{q}}) = 1 - (1 - \widehat{G}_{\mathbf{k}})(1 - \widehat{G}_{\mathbf{p}})(1 - \widehat{G}_{\mathbf{q}}), \quad (9)$$

where $0 < f_n \leq 1$ ($n = 4, 6$). On the other hand, the \mathbf{k} -th Fourier mode of the diffusive term is multiplied by

$$h_4^\gamma(\widehat{G}_{\mathbf{k}}) = 1 + 1/2(1 + \gamma)(1 - \widehat{G}_{\mathbf{k}})^2 \quad (10)$$

where $h_4^\gamma \geq 1$. Moreover, since for a generic symmetric convolution filter (see [6], for instance), $\widehat{G}_{\mathbf{k}} = 1 - \alpha^2|\mathbf{k}|^2 + \mathcal{O}(\alpha^4)$ with $\alpha^2 = \epsilon^2/24$, the functions f_4^γ and h_4^γ can be approximated by $f_4^\gamma \approx 1 - 1/2(1 + \gamma)\alpha^4(|\mathbf{k}|^2|\mathbf{p}|^2 + |\mathbf{k}|^2|\mathbf{q}|^2 + |\mathbf{p}|^2|\mathbf{q}|^2)$ and $h_4^\gamma \approx 1 + 1/2(1 + \gamma)\alpha^4|\mathbf{k}|^4$, respectively. Therefore, the interactions between large scales of motion ($\epsilon|\mathbf{k}| < 1$) approximate the NS dynamics up to $\mathcal{O}(\epsilon^4)$.

2.2 Finding a criterion for f_4^γ

On the other hand, taking the curl of Eq.(3) leads to

$$\partial_t\boldsymbol{\omega} + \mathcal{C}_4^\gamma(\mathbf{u}, \boldsymbol{\omega}) = \mathcal{C}_4^\gamma(\boldsymbol{\omega}, \mathbf{u}) + \mathcal{D}_4^\gamma\boldsymbol{\omega}. \quad (11)$$

This equation resembles the vorticity equation that results from the NS equations: the only difference is that \mathcal{C} and \mathcal{D} are replaced by their regularizations \mathcal{C}_4^γ and \mathcal{D}_4^γ , respectively. If it happens that the vortex stretching term, $\mathcal{C}_4^\gamma(\boldsymbol{\omega}, \mathbf{u})$, in Eq.(11) is so strong that the dissipative term, $\mathcal{D}_4^\gamma\boldsymbol{\omega}$, cannot prevent the intensification of vorticity, smaller vortical structures are produced. Left-multiplying the vorticity transport Eq.(11) by $\boldsymbol{\omega}$, we can obtain the evolution of $|\boldsymbol{\omega}|^2$. In this way, the vortex-stretching and dissipation term contributions to $\partial_t|\boldsymbol{\omega}|^2$ result

$$\boldsymbol{\omega} \cdot \mathcal{C}_4^\gamma(\boldsymbol{\omega}, \mathbf{u}) \quad \text{and} \quad \boldsymbol{\omega} \cdot \mathcal{D}_4^\gamma\boldsymbol{\omega}, \quad (12)$$

respectively. In order to prevent local intensification of vorticity, dissipation must dominate the vortex-stretching term contribution at the smallest grid scale, $|\mathbf{k}_c| = \sqrt{3}\pi/h$. In spectral space, this requirement leads to the following inequality

$$\frac{1}{2} \frac{(\hat{\boldsymbol{\omega}}_{\mathbf{k}_c} \cdot \mathcal{C}_4^\gamma(\boldsymbol{\omega}, \mathbf{u})_{\mathbf{k}_c}^* + \mathcal{C}_4^\gamma(\boldsymbol{\omega}, \mathbf{u})_{\mathbf{k}_c} \cdot \hat{\boldsymbol{\omega}}_{\mathbf{k}_c}^*)}{\hat{\boldsymbol{\omega}}_{\mathbf{k}_c} \cdot \hat{\boldsymbol{\omega}}_{\mathbf{k}_c}^*} \leq h_4^\gamma(\hat{G}_{\mathbf{k}_c}) \nu \mathbf{k}_c^2, \quad (13)$$

where the vortex-stretching term, $\mathcal{C}_4^\gamma(\boldsymbol{\omega}, \mathbf{u})_{\mathbf{k}_c}$, is given by

$$\mathcal{C}_4^\gamma(\boldsymbol{\omega}, \mathbf{u})_{\mathbf{k}_c} = \sum_{\mathbf{p}+\mathbf{q}=\mathbf{k}_c} f_4^\gamma(\hat{G}_{\mathbf{k}_c}, \hat{G}_{\mathbf{p}}, \hat{G}_{\mathbf{q}}) \hat{\boldsymbol{\omega}}_{\mathbf{p}} i \mathbf{q} \hat{\mathbf{u}}_{\mathbf{q}}. \quad (14)$$

Note that $f_4^\gamma(\hat{G}_{\mathbf{k}_c}, \hat{G}_{\mathbf{p}}, \hat{G}_{\mathbf{q}})$ depends on the filter length ϵ and, in general, on the wavevectors \mathbf{p} and $\mathbf{q} = \mathbf{k}_c - \mathbf{p}$. This makes very difficult to control the damping effect because f_4^γ cannot be taken out of the summation in (14). To avoid this, filters should be constructed from the requirement that the damping effect of all the triadic interactions at the smallest scale must be virtually independent of the interacting pairs, *i.e.*

$$f_4^\gamma(\hat{G}_{\mathbf{k}_c}, \hat{G}_{\mathbf{p}}, \hat{G}_{\mathbf{q}}) \approx f_4^\gamma(\hat{G}_{\mathbf{k}_c}). \quad (15)$$

This is a crucial property to control the subtle balance between convection and diffusion in order to stop the vortex-stretching mechanism. This point was addressed in detail in [7]. Then, the overall damping effect at the smallest grid scale, $H_4(\hat{G}_{\mathbf{k}_c})$, follows straightforwardly

$$H_4(\hat{G}_{\mathbf{k}_c}) = \frac{f_4^\gamma(\hat{G}_{\mathbf{k}_c})}{h_4^\gamma(\hat{G}_{\mathbf{k}_c})} = \frac{2\nu \mathbf{k}_c^2 \hat{\boldsymbol{\omega}}_{\mathbf{k}_c} \cdot \hat{\boldsymbol{\omega}}_{\mathbf{k}_c}^*}{\hat{\boldsymbol{\omega}}_{\mathbf{k}_c} \cdot \mathcal{C}(\boldsymbol{\omega}, \mathbf{u})_{\mathbf{k}_c}^* + \mathcal{C}(\boldsymbol{\omega}, \mathbf{u})_{\mathbf{k}_c} \cdot \hat{\boldsymbol{\omega}}_{\mathbf{k}_c}^*}, \quad (16)$$

with the condition that $0 < H_4(\hat{G}_{\mathbf{k}_c}) \leq 1$. Notice that $h_4^\gamma(\hat{G}_{\mathbf{k}_c}) = 2 - f_4^\gamma(\hat{G}_{\mathbf{k}_c})$; therefore, the damping function $f_4^\gamma(\hat{G}_{\mathbf{k}_c})$ reads

$$f_4^\gamma(\hat{G}_{\mathbf{k}_c}) = \frac{2H_4(\hat{G}_{\mathbf{k}_c})}{1 + H_4(\hat{G}_{\mathbf{k}_c})}. \quad (17)$$

2.3 Practical re-definition of f_4^γ

In Eq.(7), the f_4^γ was defined as

$$f_4^\gamma(\hat{G}_{\mathbf{k}}, \hat{G}_{\mathbf{p}}, \hat{G}_{\mathbf{q}}) = 1/2 \{(1 + \gamma)f_4 + (1 - \gamma)f_6\}(\hat{G}_{\mathbf{k}}, \hat{G}_{\mathbf{p}}, \hat{G}_{\mathbf{q}}), \quad (18)$$

however, in general, this expression is not very practical because it implies (i) the calculation of f_6 given in Eq.(9) and (ii) the re-construction of discrete linear filters that fulfill the property given in Eq.(15). The latter is especially difficult since those filters

should also be γ -dependent. Alternatively, we propose to re-use the discrete linear filters proposed in [7] for the f_4 damping function. Hence, Eq.(18) needs to be simplified to be expressed in terms of f_4 . Two options have been analyzed. Namely,

$$f_4^{\gamma,1}(\widehat{G}_{\mathbf{k}}, \widehat{G}_{\mathbf{p}}, \widehat{G}_{\mathbf{q}}) = 1/2 \{(1 + \gamma)f_4 + (1 - \gamma)\} (\widehat{G}_{\mathbf{k}}, \widehat{G}_{\mathbf{p}}, \widehat{G}_{\mathbf{q}}) = \tilde{\gamma}f_4(\widehat{G}_{\mathbf{k}}, \widehat{G}_{\mathbf{p}}, \widehat{G}_{\mathbf{q}}) + (1 - \tilde{\gamma}), \quad (19)$$

$$f_4^{\gamma,2}(\widehat{G}_{\mathbf{k}}, \widehat{G}_{\mathbf{p}}, \widehat{G}_{\mathbf{q}}) = 1/2 \{(1 + \gamma)f_4 + (1 - \gamma)f_4\} (\widehat{G}_{\mathbf{k}}, \widehat{G}_{\mathbf{p}}, \widehat{G}_{\mathbf{q}}) = f_4(\widehat{G}_{\mathbf{k}}, \widehat{G}_{\mathbf{p}}, \widehat{G}_{\mathbf{q}}), \quad (20)$$

where $\tilde{\gamma} = 1/2(1 + \gamma)$. The former assumes that $f_4 \approx f_6$ whereas the latter assumes $f_6 \approx 1$. At the smallest grid scale, \mathbf{k}_c , and assuming that the equality Eq.(15) is satisfied they result

$$f_4^{\gamma,1}(\widehat{G}_{\mathbf{k}_c}, \widehat{G}_{\mathbf{k}_c}, 1) = \tilde{\gamma}(2\widehat{G}_{\mathbf{k}_c} - \widehat{G}_{\mathbf{k}_c}^2) + (1 - \tilde{\gamma}), \quad (21)$$

$$f_4^{\gamma,2}(\widehat{G}_{\mathbf{k}_c}, \widehat{G}_{\mathbf{k}_c}, 1) = (2\widehat{G}_{\mathbf{k}_c} - \widehat{G}_{\mathbf{k}_c}^2). \quad (22)$$

Then, recalling that h_4^γ is given by $h_4^\gamma(\widehat{G}_{\mathbf{k}}) = 1 + 1/2(1 + \gamma)(1 - \widehat{G}_{\mathbf{k}})^2$ (see Eq. 10), the relation between $h_4^\gamma(\widehat{G}_{\mathbf{k}_c})$ and $f_4^\gamma(\widehat{G}_{\mathbf{k}_c})$ reads

$$h_4^{\gamma,1}(\widehat{G}_{\mathbf{k}_c}) = 2(1 + \tilde{\gamma}) - f_4^{\gamma,1}(\widehat{G}_{\mathbf{k}_c}), \quad (23)$$

$$h_4^{\gamma,2}(\widehat{G}_{\mathbf{k}_c}) = 1 + \tilde{\gamma}(1 - f_4^{\gamma,2}(\widehat{G}_{\mathbf{k}_c})), \quad (24)$$

and $f_4^{\gamma,1}(\widehat{G}_{\mathbf{k}_c})$ and $f_4^{\gamma,2}(\widehat{G}_{\mathbf{k}_c})$ in terms of $H_4(\widehat{G}_{\mathbf{k}_c})$ follow

$$f_4^{\gamma,1}(\widehat{G}_{\mathbf{k}_c}) = \frac{2(1 + \tilde{\gamma})H_4(\widehat{G}_{\mathbf{k}_c})}{1 + H_4(\widehat{G}_{\mathbf{k}_c})}, \quad f_4^{\gamma,2}(\widehat{G}_{\mathbf{k}_c}) = \frac{(1 + \tilde{\gamma})H_4(\widehat{G}_{\mathbf{k}_c})}{1 + \tilde{\gamma}H_4(\widehat{G}_{\mathbf{k}_c})}. \quad (25)$$

Finally, from a practical point-of-view it is more appropriate to find the relations of $f_4(\widehat{G}_{\mathbf{k}_c})$ in terms of $H_4(\widehat{G}_{\mathbf{k}_c})$

$$f_4(\widehat{G}_{\mathbf{k}_c}) = \frac{f_4^{\gamma,1}(\widehat{G}_{\mathbf{k}_c}) - (1 - \tilde{\gamma})}{\tilde{\gamma}} = \frac{(1 + \tilde{\gamma})H_4(\widehat{G}_{\mathbf{k}_c}) - (1 - \tilde{\gamma})}{\tilde{\gamma}(1 + H_4(\widehat{G}_{\mathbf{k}_c}))}, \quad (26)$$

$$f_4(\widehat{G}_{\mathbf{k}_c}) = f_4^{\gamma,2}(\widehat{G}_{\mathbf{k}_c}) = \frac{(1 + \tilde{\gamma})H_4(\widehat{G}_{\mathbf{k}_c})}{1 + \tilde{\gamma}H_4(\widehat{G}_{\mathbf{k}_c})}, \quad (27)$$

where $f_4(\widehat{G}_{\mathbf{k}_c}) \approx (2\widehat{G}_{\mathbf{k}_c} - \widehat{G}_{\mathbf{k}_c}^2)$. The first approach relies on the assumption that $f_6 \approx 1$. For a wide range of frequencies this is probably a reasonable approximation since $f_6 \approx 1 - \alpha^6|\mathbf{k}|^2|\mathbf{p}|^2|\mathbf{q}|^2$ whereas $f_4 \approx 1 - \alpha^4(|\mathbf{k}|^2|\mathbf{p}|^2 + |\mathbf{k}|^2|\mathbf{q}|^2 + |\mathbf{p}|^2|\mathbf{q}|^2)$. However, the foregoing analysis is localized at the smallest grid scale, \mathbf{k}_c , where this assumption is not correct. On the other hand, the second approach assumes the $f_6 \approx f_4$. In Figure 1, the dependence of $f_4(\widehat{G}_{\mathbf{k}_c})$ respect to $H_4(\widehat{G}_{\mathbf{k}_c})$ is displayed. Only the second approach, $f_6(\widehat{G}_{\mathbf{k}_c}) \approx f_4(\widehat{G}_{\mathbf{k}_c})$, shows an appropriate behavior: (i) $0 \leq f_4(\widehat{G}_{\mathbf{k}_c}) \leq 1$ irrespectively of the value of $\tilde{\gamma}$ and

$H_4(\widehat{G}_{\mathbf{k}_c})$ (ii) and $f_4(\widehat{G}_{\mathbf{k}_c}) = 0$ for $H_4(\widehat{G}_{\mathbf{k}_c}) = 0$ and $f_4(\widehat{G}_{\mathbf{k}_c}) = 1$ for $H_4(\widehat{G}_{\mathbf{k}_c}) = 1$ for any value of $\tilde{\gamma}$. Notice that for $\tilde{\gamma} < 1$ and $H_4(\widehat{G}_{\mathbf{k}_c}) < (1 - \tilde{\gamma})/(\tilde{\gamma} + 1)$, the expression (26) leads to negative values of $f_4(\widehat{G}_{\mathbf{k}_c})$. An example thereof is given in Figure 1 (top, left) where $\tilde{\gamma} = 0.5$ and $f_4(\widehat{G}_{\mathbf{k}_c}) < 0$ for $H_4(\widehat{G}_{\mathbf{k}_c}) < 1/3$. For all the above-mentioned reasons we adopt the second approach, *i.e.* $f_6(\widehat{G}_{\mathbf{k}_c}) \approx f_4(\widehat{G}_{\mathbf{k}_c})$; therefore, the relation between $f_4(\widehat{G}_{\mathbf{k}_c})$ and $H_4(\widehat{G}_{\mathbf{k}_c})$ is given by Eq.(27) whereas $h_4^\gamma(\widehat{G}_{\mathbf{k}_c})$ is given by Eq.(24).

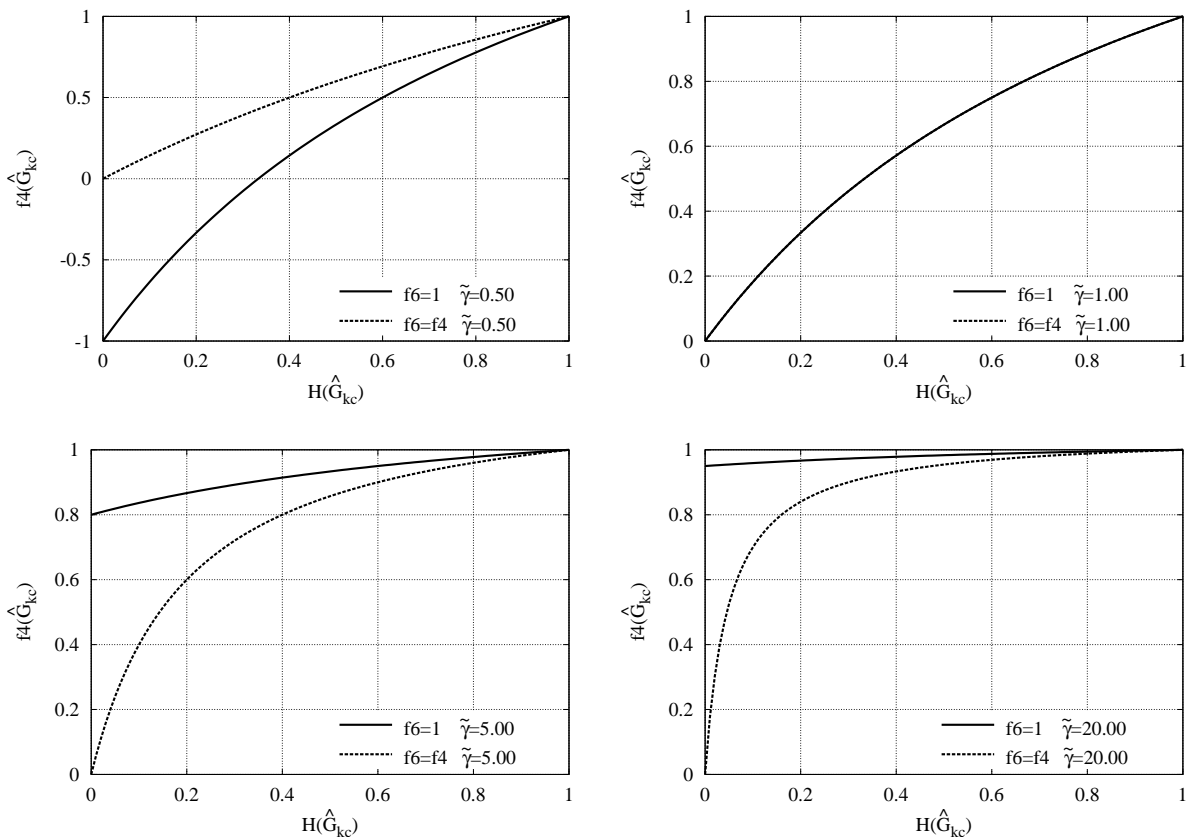


Figure 1: Dependence of $f_4(\widehat{G}_{\mathbf{k}_c})$ respect to $H_4(\widehat{G}_{\mathbf{k}_c})$ for both approaches ($f_6(\widehat{G}_{\mathbf{k}_c}) \approx 1$ and $f_6(\widehat{G}_{\mathbf{k}_c}) \approx f_4(\widehat{G}_{\mathbf{k}_c})$) and for different values of $\tilde{\gamma}$.

3 ON THE DETERMINATION OF γ

A criterion to determine the local filter length, ϵ , has been presented in the previous section. Then, the only parameter that still needs to be determined in Eq.(3) is the constant γ . At this point, the 'optimal' value of γ could be determined by means of a trial-and-error numerical procedure. Alternatively, the constant γ can be obtained by assuming that the smallest grid scale $k_c = |\mathbf{k}_c| = \sqrt{3}\pi/h$ lies within the inertial range for a classical Kolmogorov energy spectrum $E(k) = C_K \epsilon^{2/3} k^{-5/3}$. In such a case, and

recalling that $\widehat{G}_{\mathbf{k}} = 1 - \alpha^2|\mathbf{k}|^2 + \mathcal{O}(\alpha^4)$, the total dissipation for $k_T \leq k \leq k_c$ can be approximated by the contribution of the following two terms

$$\mathcal{D}_\nu \equiv \nu \int_{k_T}^{k_c} k^2 E(k) dk \quad \mathcal{D}_\nu'' \equiv \nu \int_{k_T}^{k_c} k^4 \alpha^4 E(k) dk, \quad (28)$$

where \mathcal{D}_ν is the physical viscous dissipation and \mathcal{D}_ν'' is the additional dissipation introduced by the hyper-viscosity term, $(\mathcal{D}\mathbf{u})'$. Hence, integration for a Kolmogorov energy spectrum, the total dissipation within the range $k_T \leq k \leq k_c$ is given by

$$\mathcal{D}_\nu + \tilde{\gamma}\mathcal{D}_\nu'' = \frac{3\nu}{16} C_K \varepsilon^{2/3} \left\{ (4 + \tilde{\gamma}\alpha^4 k_c^4) k_c^{4/3} - (4 + \tilde{\gamma}\alpha^4 k_T^4) k_T^{4/3} \right\}, \quad (29)$$

where $\tilde{\gamma} = 1/2(1 + \gamma)$ has been introduced here for the sake of simplicity. At the tail of the spectrum the following

$$\tilde{H}_4 \approx \frac{\mathcal{D}_\nu + \tilde{\gamma}\mathcal{D}_\nu''}{\varepsilon}, \quad (30)$$

represents the ratio between the total dissipation and the energy transferred from scales larger than k_T to the tail of the spectrum. Let us assume that $\tilde{H}_4 = \mathcal{O}(H_4(\widehat{G}_{\mathbf{k}_c}))$ where the overall damping at the smallest grid scale, $H_4(\widehat{G}_{\mathbf{k}_c})$, is given by Eq.(16). In order to apply the method in a physical domain in \mathbb{R}^3 , the following (equivalent) bounding was proposed in [4]

$$H_4(\widehat{G}_{\mathbf{k}_c}) = \min \{ \lambda_\Delta \nu Q / |R|, 1 \}, \quad (31)$$

where $R = -1/3tr(S^3) = -det(S) = -\lambda_1\lambda_2\lambda_3$ and $Q = -1/2tr(S^2) = -1/2(\lambda_1^2 + \lambda_2^2 + \lambda_3^2)$ are the invariants of $S = 1/2(\nabla\mathbf{u} + \nabla\mathbf{u}^T)$, respectively, and $\lambda_1 \leq \lambda_2 \leq \lambda_3$ are the eigenvalues of S . $\lambda_\Delta < 0$ is the largest (smallest in absolute value) non-zero eigenvalue of the Laplacian operator Δ on an arbitrary part of the flow domain Ω with periodic boundary conditions. If we consider that the domain Ω is a box of volume h , then $\lambda_\Delta = -(\pi/h)^2$. In a numerical simulation h would be related with the local grid size.

However, at this point it is more suitable to express it in terms of the invariant Q . To do so, we simply notice that the three eigenvalues of S can be computed analytically, *i.e.* $\lambda_i = -|S|\sqrt{1/3} \cos(\theta/3 - 2\pi(i-1)/3)$, $i = 1, 2, 3$, where $|S| = \sqrt{-4Q}$ and the angle θ is given by $\theta = \arccos\{1/2R/(-\frac{1}{3}Q)^{3/2}\}$. Since S is symmetric, the eigenvalues must be real-valued, $\lambda_i \in \mathbb{R}$; therefore, the invariants Q and R satisfy $27R^2 + 4Q^3 \leq 0$. Hence, $\theta \in [0, \pi]$ and the ratio $|R|/-Q$ can be bounded in terms of the invariant Q , *i.e.* $0 \leq |R|/-Q \leq \sqrt{-4Q/27}$. Then, plugging this into Eq.(31) leads to

$$1 \geq H_4(\widehat{G}_\pi) \geq -\sqrt{\frac{27}{4}} \frac{\lambda_\Delta \nu}{\sqrt{-Q}}. \quad (32)$$

On the other hand, for a classical Kolmogorov energy spectrum, the ensemble averaged invariant Q is approximately given by

$$\langle Q \rangle = -\frac{1}{4} \int_0^{k_c} k^2 E(k) dk \approx -\frac{3}{16} C_K \varepsilon^{2/3} k_c^{4/3}. \quad (33)$$

Finally, combining Eqs.(32) and (33), the energy balance given by Eq.(30) results

$$\frac{-12\lambda_\Delta\nu\varepsilon}{\sqrt{C_K\varepsilon^{2/3}k_c^{4/3}}} \lesssim \mathcal{D}_\nu + \tilde{\gamma}\mathcal{D}_\nu'' \quad (34)$$

Then, plugging Eq.(29) and recalling that $\lambda_\Delta = -3(\pi/h)^2$, $k_c = \sqrt{3}\pi/h$ and $\alpha \approx k_c^{-1}$, the previous expression simplifies

$$1 \lesssim \frac{C_K^{3/2}}{32} \left\{ (4 + \tilde{\gamma}) - \left(4 + \tilde{\gamma} \left(\frac{k_T}{k_c} \right)^4 \right) \left(\frac{k_T}{k_c} \right)^{4/3} \right\}. \quad (35)$$

Since $k_c > k_T$ we can consider that $4 \gg \tilde{\gamma}(k_T/k_c)^4$ to obtain a proper bound for $\tilde{\gamma}$,

$$\tilde{\gamma} \gtrsim 4 \left\{ 8C_K^{-3/2} - \left(1 - \left(\frac{k_T}{k_c} \right)^{4/3} \right) \right\} \approx 4 \left(8C_K^{-3/2} - 1 \right). \quad (36)$$

Hence, for a Kolmogorov constant of $C_K \approx 1.58$ [8] it leads to $\tilde{\gamma} \gtrsim 12.1$ ($\gamma \gtrsim 23.2$). To confirm whether this is a proper estimation of $\tilde{\gamma}$ numerical experiments are required.

4 NUMERICAL EXPERIMENTS

The $\{\mathcal{CD}\}_4^\gamma$ -regularization has been proposed in the previous sections. In short, the original NS equations (1) are replaced by the smoother approximation given in Eqs.(3) where $\mathcal{C}_4^\gamma(\mathbf{u}_\epsilon, \mathbf{u}_\epsilon)$ and $\mathcal{D}_4^\gamma\mathbf{u}_\epsilon$ are given by Eqs.(4). Then, the criteria to determine the damping factor of the discrete linear filter at the smallest grid scale are respectively given by Eq.(16) (spectral space) and Eq.(31) (physical space). Regarding the implementation of $\mathcal{C}_4^\gamma(\mathbf{u}_\epsilon, \mathbf{u}_\epsilon)$, we follow the approach proposed in Section 2.3; therefore, the damping function at the smallest grid scale, $f_4^\gamma(\hat{G}_{\mathbf{k}_c})$, with the overall damping, $H_4(\hat{G}_{\mathbf{k}_c})$, is given by Eq.(27) whereas $h_4^\gamma(\hat{G}_{\mathbf{k}})$ is still given by Eq.(10). Finally, the value of $\tilde{\gamma}$ has been approximately bounded by Eq.(36). In this section several numerical experiments are carried out to assess the performance of the proposed method.

4.1 Burgers' equation

The numerical simulation of the 1D Burgers' equation

$$\partial_t u + \mathcal{C}(u, u) = \frac{1}{Re} \partial_{xx}^2 u + f, \quad (37)$$

on an interval $x \in (0, 2\pi)$ with periodic boundary conditions has been chosen as a first test-case to assess the performance of the proposed $\{\mathcal{CD}\}_4^\gamma$ -regularization method. Despite its simplicity, important aspects of the 3D NS equations remain (see [9], for instance). Note that now the convective term is given by $\mathcal{C}(u, u) = u\partial_x u$. In Fourier space, it reads

$$\partial_t \hat{u}_k + \sum_{p+q=k} \hat{u}_p i q \hat{u}_q = -\frac{k^2}{Re} \hat{u}_k + F_k, \quad (38)$$

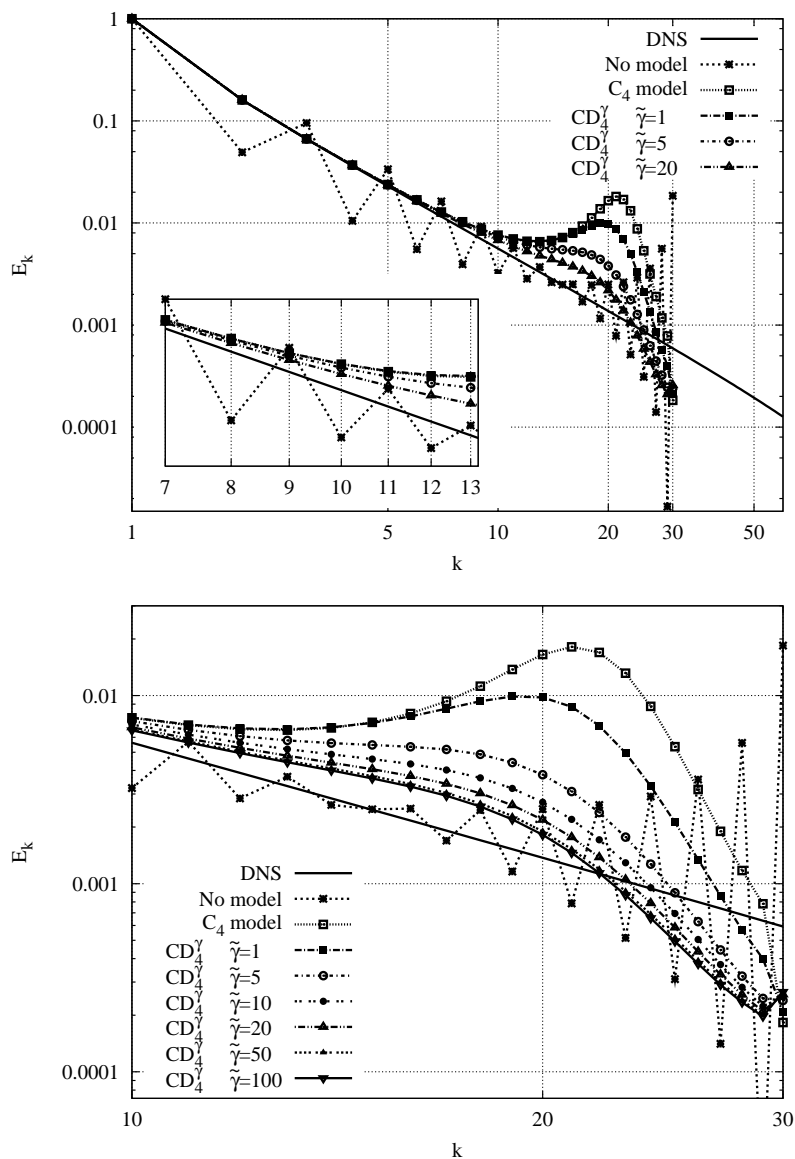


Figure 2: Left: energy spectra of the steady-state solution of the Burgers' equation at $Re = 100$ with and without modeling, for $k_c = 30$. Direct comparison with the DNS reference solution (solid line) with $k_c = 300$. Right: zoom of the tail of the spectra for different values of $\tilde{\gamma}$ from 0 to 100.

where \hat{u}_k denotes the k -th Fourier mode of $u(x, t) \in \mathbb{R}$. The initial conditions are set to $\hat{u}_k = k^{-1}$ whereas the forcing term vanishes $F_k = 0$ for $k > 1$ and F_1 forces $\partial_t \hat{u}_1 = 0$. For details about the spectral numerical algorithm and the discrete linear filters the reader is referred to [7]. Results obtained with and without regularization for $k_c = 30$ are displayed in Figure 2 and compared with the DNS reference solution (solid line) obtained with $k_c = 300$. Clearly, the direct simulation without model with $k_c = 30$ is not able to

capture the physics. At high wavenumbers, the energy is not dissipated enough; therefore, it is reflected back towards the larger scales. The zoom in Figure 2 (left) shows that the direct simulation with $k_c = 30$ is substantially different from the DNS even for low wavenumbers. Regarding the effect of $\tilde{\gamma}$, different values have been tested. As expected, the \mathcal{C}_4 solution, that corresponds to $\tilde{\gamma} = 0$, displays a hump at the tail of the spectrum. This effect was already observed in [7]. Figure 2 (right) shows how this undesirable effect tends to attenuate for increasing values of $\tilde{\gamma}$. Even more important, it seems to reach an asymptotic solution for $\tilde{\gamma} \gtrsim 100$. This is in a fairly good agreement with the estimation given by Eq.(36). Notice that for the Burgers' equation $C_K \approx 0.452$; therefore, it leads to $\tilde{\gamma} \gtrsim 101.3$. Similar results have been obtained at higher Re .

4.2 Forced homogeneous isotropic turbulence

The simulation of forced homogeneous isotropic turbulence has been chosen as the second test-case. The code is pseudo-spectral and uses the 3/2 dealiasing rule. Filters proposed in [7] are applied in spectral space. The total amount of energy in the first two modes is kept constant following the approach proposed in [10]. Figure 3 (left) displays the results at $Re_\lambda \approx 72$ for a box size of 16^3 for different values of $\tilde{\gamma}$ from 0 up to 30. As expected, the original hump displayed for $\tilde{\gamma} = 0$ attenuates for increasing values of $\tilde{\gamma}$. Moreover, the lower bound for $\tilde{\gamma}$ given by Eq.(36) is in a fairly good agreement with these numerical tests. Even more important, for $\tilde{\gamma}$ bigger than a certain value, the results are virtually independent on the value of $\tilde{\gamma}$.

Figure 3 (right) displays the results obtained for a box size of 64^3 and $Re_\lambda \approx 202$. In this case, the energy-containing and dissipative scales are clearly separated by an inertial range. Again, the hump at the tail of the spectrum attenuates for increasing values of $\tilde{\gamma}$. More importantly, the inertial range is well predicted only for those cases with $\tilde{\gamma} \gtrsim 14$, in relatively good agreement with the lower bound given by Eq.(36).

5 CONCLUDING REMARKS AND FUTURE RESEARCH

Despite the rapidly growing computing power and the availability of efficient parallel algorithms, in the foreseeable future, numerical simulations of turbulent flows will have to resort to models of the small scales for which numerical resolution is not available. The most popular example thereof is the Large-Eddy Simulation (LES). Alternatively, regularizations of the non-linear convective term basically reduce the transport towards the small scales: the convective term in the Navier-Stokes (NS) equations is replaced by a smoother approximation. In the present work, we have proposed the $\{\mathcal{CD}\}_4^\gamma$ -regularization of the NS equations: the convective and diffusive operators in the NS equations (1) are replaced by the $\mathcal{O}(\epsilon^4)$ -accurate smooth approximation given by Eq.(4). This linkage follows from (approximately) restoring the Galilean invariance for the regularization by means of a modification of the diffusive term. Then, the only additional ingredient is a self-adjoint linear filter whose local filter length is determined from the requirement

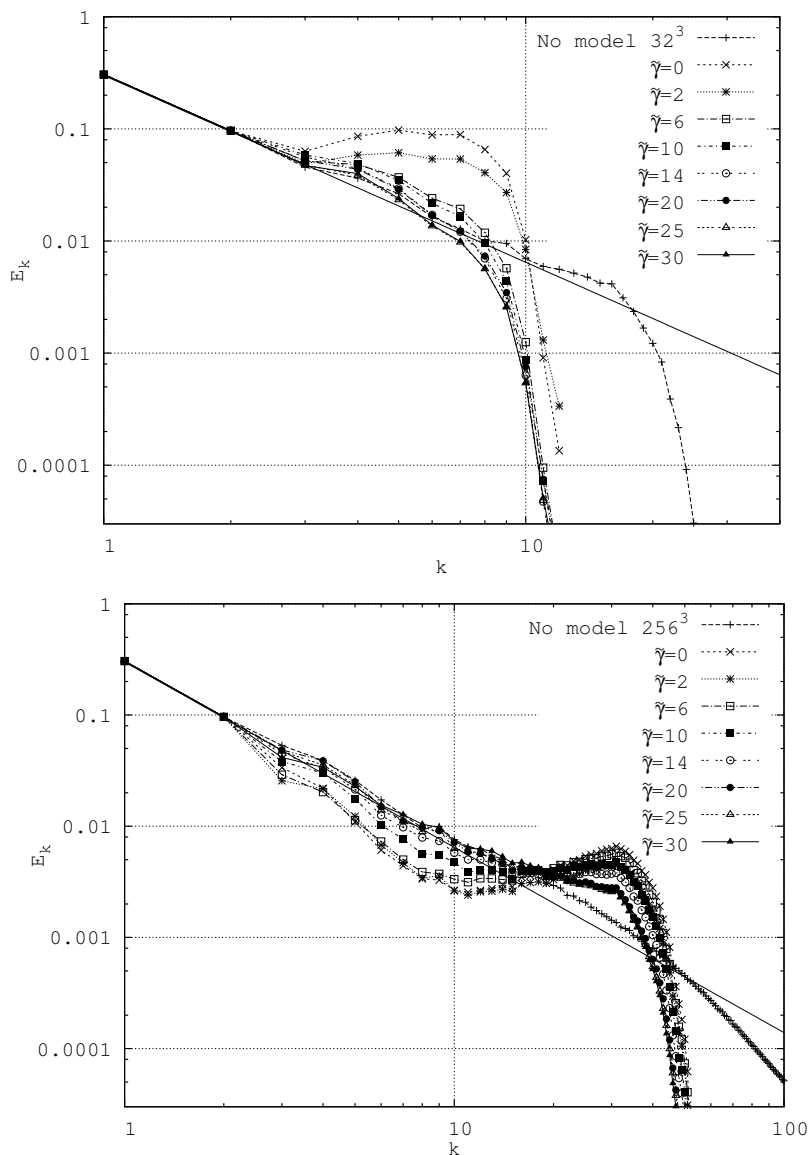


Figure 3: Energy spectra at $Re_\lambda \approx 72$ (left) and $Re_\lambda \approx 202$ (right) for different values of $\tilde{\gamma}$ from 0 up to 30.

that vortex-stretching must be stopped at the scale set by the grid via Eq.(16) provided that discrete filter satisfies Eq.(15). Regarding the parameter γ of Eq.(3), it has been approximately bounded by assuming a Kolmogorov energy spectrum. In this way, the following bound has been determined:

$$\tilde{\gamma} \gtrsim 4 \left(8C_K^{-3/2} - 1 \right), \quad (39)$$

where $\tilde{\gamma} = 1/2(1 + \gamma)$ and C_K is the Kolmogorov constant. The performance of the method has been successfully assessed through application to the Burgers' equation and a homogeneous isotropic turbulence.

ACKNOWLEDGMENTS

This work has been financially supported by the *Ministerio de Ciencia e Innovación*, Spain (ENE2010-17801), and a *Ramón y Cajal* postdoctoral contracts (RYC-2012- 11996) by the *Ministerio de Ciencia e Innovación*. Calculations have been performed on the IBM MareNostrum supercomputer at the Barcelona Supercomputing Center. The authors thankfully acknowledge these institutions.

REFERENCES

- [1] B. J. Geurts and D. D. Holm. Regularization modeling for large-eddy simulation. *Physics of Fluids*, 15:L13–L16, 2003.
- [2] J. L. Guermond, J. T. Oden, and S. Prudhomme. An interpretation of the Navier-Stokes-alpha model as a frame-indifferent Leray regularization. *Physica D*, 177:23–30, 2003.
- [3] Roel Verstappen. On restraining the production of small scales of motion in a turbulent channel flow. *Computers & Fluids*, 37:887–897, 2008.
- [4] F. X. Trias, A. Gorobets, C. D. Pérez-Segarra, and A. Oliva. DNS and regularization modeling of a turbulent differentially heated cavity of aspect ratio 5. *International Journal of Heat and Mass Transfer*, 57:171–182, 2013.
- [5] F. X. Trias, D. Folch, A. Gorobets, and A. Oliva. Spectrally-consistent regularization modeling of wind farm boundary layers. In *Conference on Modelling Fluid Flow 2012*, Budapest, Hungary, September 2012.
- [6] D. Carati, G. S. Winckelmans, and H. Jeanmart. Exact expansions for filtered-scales modelling with a wide class of LES filters. In *Direct and Large-Eddy Simulation III*, pages 213–224. Kluwer, 1999.
- [7] F. X. Trias and R. W. C. P. Verstappen. On the construction of discrete filters for symmetry-preserving regularization models. *Computers & Fluids*, 40:139–148, 2011.
- [8] D. A. Donzis and K. R. Sreenivasan. The bottleneck effect and the Kolmogorov constant in isotropic turbulence. *Journal of Fluid Mechanics*, 657:171–188, 2010.
- [9] S. Basu. Can the dynamic eddy-viscosity class of subgrid-scale models capture inertial-range properties of Burgers turbulence? *Journal of Turbulence*, 10(12):1–16, 2009.
- [10] S. Chen, G. D. Doolen, R. H. Kraichnan, and Z. She. On statistical correlations between velocity increments and locally averaged dissipation in homogeneous turbulence. *Physics of Fluids A*, 5:458, 1993.